Inorg. Chem. **2009**, *48*, 1566−1576

Mononuclear Ferrocenophane Structural Motifs with Two Thiourea Arms Acting as a Dual Binding Site for Anions and Cations

Francisco Otón,[†] Arturo Espinosa,[†] Alberto Tárraga,*[,†] Imma Ratera,[‡] Klaus Wurst,[§] Jaime Veciana,*[,‡] and Pedro Molina*[,†]

Departamento de Química Orgánica, Facultad de Química, Campus de Espinardo, Universidad de Murcia, E-30100 Murcia, Spain, Institut de Ciencia de Materials de Barcelona (CSIC)/ CIBER-BBN, Bellaterra, E-08193 Barcelona, Spain, and Institut für Allgemeine Anorganische and Teoretische, Universität Innsbrück, Innrain 52a, A-6020 Innsbrück, Austria

Received October 2, 2008

The synthesis of a new type of mononuclear ferrocenophane-based thiourea, in which the ferrocene moiety is simultaneously attached to two thiourea groups directly from 1,1′-bis(isothiocyanato)ferrocene, is reported. These nitrogen-rich structural motifs show remarkable ion-sensing properties because of the presence of the redox active ferrocene unit and the thiourea bridges, which unexpectedly act as a dual binding site for anions and metal ions. They display a selective downfield shift of the thiourea protons and a remarkable cathodic shift of the ferrocene/ferrocenium redox couple with F^-, AcO^-, $H_2PO_4^-$, and $HP_2O_7^{3-}$ anions, whereas the selective recognition of Hg^{2+} metal cations is achieved either by electrochemical or by spectral measurements. The preferred binding modes are proposed for the most representative complexes by means of density functional theory based theoretical calculations showing the Janus-like faces of the receptor.

Introduction

Artificial neutral receptors for anions became attractive targets for study because of their analogy to natural systems and because their selectivities were higher than in the case of charged ligands. A number of anion receptors have been reported which have various functional groups acting as anion binding sites. In neutral hosts, anion binding is usually accomplished through hydrogen bonds, and in this context, thiourea subunits are currently used in the design of neutral receptors for anions, owing to their ability to act as H-bond donors.[1]

The redox behavior of a ferrocene moiety in the selective electrochemical sensing of anions has also been exploited.[2] In particular, acyclic and macrocyclic amide- and urea-functionalized ferrocene derivatives have all been shown to undergo substantial cathodic perturbations of the respective metallocene redox couple in the presence of a variety of anions of biological and environmental importance.[1b,2,3] However, there is only one example of thiourea/ferrocene redox-active cationophore, although it could not be exploited in the selective electrochemical sensing of anions.[4]

Regarding the cation-sensing properties of the thiourea functionality and on the basis of the strong thiophilic affinity of Hg(II), some selective chemodosimeters for Hg(II) utiliz-

* To whom correspondence should be addressed. E-mail: pmolina@um.es (P.M.), atarraga@um.es (A.T.), vecianaj@icmab.es (J.V.).
[†] Universidad de Murcia.
[‡] Institut de Ciéncia de Materials de Barcelona (CSIC).
[§] Universität Innsbrück.

(1) (a) Gale, P. A. *Coord. Chem. Rev.* **2003**, *240*, 1–226. (b) Beer, P. D.; Gale, P. A. *Angew. Chem., Int. Ed.* **2001**, *40*, 486–516. (c) Schmidtchen, F. P.; Berger, M. *Chem. Rev.* **1997**, *97*, 1609–1646. (d) Sessler, J. L.; Gale, P. A.; Cho, W.-S. *Anion Receptor Chemistry*; RSC Publishing: Cambridge, 2006, pp 193−202. (e) Gunlaugsson, T.; Glynn, M.; Tocci, G. M.; Kruger, P. E.; Pfeffer, F. M. *Coord. Chem. Rev.* **2006**, *250*, 3094–3117.

(2) (a) Beer, P. D.; Cadman, J. *Coord. Chem. Rev.* **2000**, *205*, 131–155. (b) Beer, P. D.; Hayes, E. J. *Coord. Chem. Rev.* **2003**, *240*, 167–189. (c) Beer, P. D.; Bayly, S. R. *Top. Curr. Chem.* **2005**, *255*, 125–162.

(3) (a) Otón, F.; Tárraga, A.; Velasco, M. D.; Espinosa, A.; Molina, P. *Chem. Commun.* **2004**, 1658–1659. (b) Otón, F.; Tárraga, A.; Velasco, M. D.; Molina, P. *Dalton Trans.* **2005**, 1159–1161. (c) Otón, F.; Tárraga, A.; Espinosa, A.; Velasco, M. D.; Bautista, D.; Molina, P. *J. Org. Chem.* **2005**, *70*, 6603–6608. (d) Otón, F.; Tárraga, A.; Espinosa, A.; Velasco, M. D.; Molina, P. *J. Org. Chem.* **2006**, *71*, 4590–4598. (e) Otón, F.; Tárraga, A.; Espinosa, A.; Velasco, M. D.; Molina, P. *Dalton Trans.* **2006**, 3685–3692.

(4) Beer, P. D.; Cavis, J. J.; Drillma-Milgrom, A.; Szemes, F. *Chem. Commun.* **2002**, 1716–1717.

10.1021/ic801879x CCC: $40.75
Published on Web 01/22/2009

ing desulfurization reaction of thioureas have been reported.[5] However, no examples dealing with the use of thiourea derivatives as chemosensor molecules for metal cations have been reported, to the best of our knowledge.

Generally, anion recognition motifs are often structurally complicated and require an elaborate and sophisticated synthetic process. Therefore, the development of chemosensors capable of recognizing and sensing anions and cations at the same time is one of the most challenging fields from the viewpoint of organic and supramolecular chemistry. From this perspective, we decided to combine in a highly preorganized system the redox activity of the ferrocene moiety with the strong hydrogen-bonding ability of the thiourea groups. Despite its homoditopic nature, the unprecedented capability for binding anions and metal cations is one interesting characteristic of these new structural motifs.

Experimental Section

General Methods. All reactions were carried out under N_2 and using solvents which were dried by routine procedures. Column chromatography was performed with the use of a column of dimensions 60 × 4.5 cm and of silica gel (60 A C.C. 70−200 μm, sds) as the stationary phase. NMR spectra were recorded at 200, 300, and 400 MHz. The following abbreviations for stating the multiplicity of the signals in the NMR spectra were used: s (singlet), bs (broad singlet), d (doublet), t (triplet), bt (broad triplet), st (pseudotriplet), dt (double triplet), m (multiplet), and q (quaternary carbon). The electrospray ionization (ESI) mass spectra were recorded on an AGILENT V spectrometer. Elemental analyses were carried out on a Carlo-Erba EA-1108 analyzer. Cyclic voltammograms (CV) and Osteryoung square wave voltammograms (OSWV) were performed with a conventional three-electrode configuration consisting of platinum working and auxiliary electrodes and a saturated calomel electrode (SCE) reference electrode. The experiments were carried out with a 10^{-3} M solution of sample in dimethyl sulfoxide (DMSO) containing 0.1 M (n-$C_4H_9)_4NPF_6$ (TBAHP) as a supporting electrolyte. All of the potential values reported are relative to the Fc^+/Fc couple at room temperature. Deoxygenation of the solutions was achieved by bubbling nitrogen for at least 10 min, and the working electrode was cleaned after each run. The CVs were recorded with a scan rate increasing from 0.05 to 1.00 V s^{-1}, while the OSWVs were recorded at a scan rate of 0.1 V s^{-1} with a pulse hight of 25 mV and a step time of 50 ms. Typically, the receptor (1×10^{-3} mol) was dissolved in solvent (5 mL), and TBAHP (base electrolyte; 0.193 g) was added. The guest under investigation was then added as a 0.1 M solution in appropriate solvent using a microsyringe, while the CV properties of the solution were monitored. Ferrocene was used either as an external or internal reference both for potential calibration and for reversibility criteria. Under similar conditions, the ferrocene has $E° = 0.390$ V vs SCE, and the anodic peak−cathodic peak separation is 67 mV. Microcalorimetric titrations were carried out using an isothermal titration calorimeter, and they were performed as follows: a solution of the receptor in DMSO ($c = 1 \times 10^{-3}$ M) was prepared, and it was titrated with the appropriate alkylammonium salt at 25 °C. The original heat pulses were normalized using reference titrations carried out using the same salt solution but with pure solvent, as opposed to the solution containing the receptor. UV−vis titrations were performed as follows: a solution of the receptor in DMSO ($c = 1 \times 10^{-4}$ M) was prepared, and it was titrated with the appropriate cation salts at room temperature. The titrations were monitored using a VARIAN 5000 spectrophotometer. Crystallographic data were measured with a Nonius Kappa CCD, and the structure was solved by direct methods (SHELXS-97)[6] and refined by full-matrix least-squares methods on F^2 (SHELXL-97).[7]

Computational Details. Calculated geometries were fully optimized in the gas phase with tight convergence criteria at the density functional theory (DFT) level with the Gaussian 03 package,[8] using initially the B3LYP[9] functional. Thereafter, the resulting geometries were refined with the hybrid meta functional mPW1B95[10] that has been recommended for general purpose applications and was developed to produce a better performance where weak interactions are involved,[10b] such as those between ligands and heavy metals.[11] Comparison of calculated with experimental (X-ray diffraction crystallography) geometries was performed by computing the root-mean-square deviation (rmsd) extended over all heavy (non-H) atoms excluding solvent dimethylformamide (DMF) molecules. Unless otherwise stated, the 6-311G** basis set was used for all atoms, adding diffuse functions on donor atoms (F, O, N, and S; denoted as aug6-311G**) as well as the SDD basis set, with effective core potential, for Hg, Cd, and Pb. All reported data were obtained from these gas-phase optimized geometries by means of single-point calculations. Energy values were computed at the same level, considering solvent DMSO effects by using the Cossi and Barone's conductor-like polarizable continuum model (CPCM) modification[12] of the Tomasi's PCM formalism[13] and correcting the basis set superposition error by means of the counterpoise approach,[14] except for metal complexes because of convergence problems. All energies are uncorrected for the zero-point vibrational energy. The reduced basis set 6-311G**

(5) (a) Yang, X.-F.; Li, Y.; Bai, Q. *Anal. Chim. Acta* **2007**, *584*, 95–100. (b) Lee, M. H.; Cho, B. K.; Yoon, J.; Kim, J. S. *Org. Lett.* **2007**, *9*, 4515–4518. (c) Wu, F.-Y.; Zhao, Y.-Q.; Ji, Z.-J. *J. Fluoresc.* **2007**, *17*, 460–465. (d) Wu, J.-S.; Hwang, I.-C.; Kim, K. S.; Kim, J. S. *Org. Lett.* **2007**, *9*, 907–910.

(6) Sheldrick, G. M. *SHELXS-97, program for crystal structure solutions*; University of Göttingen: Göttingen, 1997.

(7) Sheldrick, G. M. *SHELXL-97, program for refinement of crystal structures*; University of Göttingen: Göttingen, 1997.

(8) Frisch, M. J.; Trucks, G. W.; Schlegel, H. B.; Scuseria, G. E.; Robb, M. A.; Cheeseman, J. R.; Montgomery J. A., Jr.; Vreven, T.; Kudin, K. N.; Burant, J. C.; Millam, J. M.; Iyengar, S. S.; Tomasi, J.; Barone, V.; Mennucci, B.; Cossi, M.; Scalmani, G.; Rega, N.; Petersson, G. A.; Nakatsuji, H.; Hada, M.; Ehara, M.; Toyota, K.; Fukuda, R.; Hasegawa, J.; Ishida, M.; Nakajima, T.; Honda, Y.; Kitao, O.; Nakai, H.; Klene, M.; Li, X.; Knox, J. E.; Hratchian, H. P.; Cross, J. B.; Bakken, V.; Adamo, C.; Jaramillo, J.; Gomperts, R.; Stratmann, R. E.; Yazyev, O.; Austin, A. J.; Cammi, R.; Pomelli, C.; Ochterski, J. W.; Ayala, P. Y.; Morokuma, K.; Voth, G. A.; Salvador, P.; Dannenberg, J. J.; Zakrzewski, V. G.; Dapprich, S.; Daniels, A. D.; Strain, M. C.; Farkas, O.; Malick, D. K.; Rabuck, A. D.; Raghavachari, K.; Foresman, J. B.; Ortiz, J. V.; Cui, Q.; Baboul, A. G.; Clifford, S.; Cioslowski, J.; Stefanov, B. B.; Liu, G.; Liashenko, A.; Piskorz, P.; Komaromi, I.; Martin, R. L.; Fox, D. J.; Keith, T.; Al-Laham, M. A.; Peng, C. Y.; Nanayakkara, A.; Challacombe, M.; Gill, P. M. W.; Johnson, B.; Chen, W.; Wong, M. W.; Gonzalez, C.; Pople, J. A. *Gaussian 03*, Revision B.03; Gaussian, Inc.: Wallingford, CT, 2004.

(9) Bartolottiand, L. J.; Fluchick, K. In *Reviews in Computational Chemistry*; Lipkowitz, K. B., Boyd, B. D., Eds.; VCH: New York, 1996; Vol. *7*, pp 187−216.

(10) (a) Zhao, Y.; Truhlar, D. G. *J. Phys. Chem. A* **2004**, *108*, 6908–6918. (b) Zhao, Y.; Truhlar, D. G. *J. Phys. Chem. A* **2005**, *109*, 5656–5667.

(11) For instance, see Mũniz, J.; Sansores, L. E.; Martínez, A.; Salcedo, R. *J. Mol. Struct.* **2007**, *820*, 141–147.

(12) (a) Barone, V.; Cossi, M. *J. Phys. Chem. A* **1998**, *102*, 1995–2001. (b) Cossi, M.; Rega, N.; Scalmani, G.; Barone, V. *J. Comput. Chem.* **2003**, *24*, 669–681.

(13) (a) Miertus, S.; Scrocco, E.; Tomasi, J. *J. Chem. Phys.* **1981**, *55*, 117–129. (b) Cammi, R.; Mennucci, B.; Tomasi, J. *J. Phys. Chem. A* **2000**, *104*, 5631–5637.

(14) Boys, S. F.; Bernardi, F. *Mol. Phys.* **1970**, *19*, 553–566.

(without diffuse functions), together with SDD-ecp (for Hg, Cd, and Pb), was used to perform the natural bond orbital (NBO) population analysis. Bond orders were characterized by the Wiberg's bond index (WBI)[15] and calculated with the NBO method as the sum of squares of the off-diagonal density matrix elements between atoms. The topological analysis of the electronic charge density was conducted by means of the Bader's atoms-in-molecules (AIM)[16] methodology using the AIM2000 software.[17]

Preparation of 1,1′-Bis(isothiocyanato)ferrocene 2. A well-stirred solution of 1,1′-bis(*N*-triphenylfosforanilideneamino)ferrocene **1** (0.1 g, 0.18 mmol) in CS_2 (8 mL) was heated at 45 °C under nitrogen for 10 h. Then, the solvent was removed under reduced pressure, and the remaining solid was slurried with diethyl ether and filtered. The filtrate was concentrated to dryness and recrystallized from hexane at −40 °C to give **2** (0.02 g, 25%) as a yellow solid. Mp 88−92 °C. IR (Nujol): ν = 2954, 2918, 2854, 2120, 2071, 1463, 1306, 1256, 1208, 1105, 1025, 817, 721 cm^{-1}. ^1H NMR (200 MHz, $CDCl_3$, at T = 60 °C): δ = 4.53 (st, 4H); 4.22 (st, 4H). ^{13}C NMR (50 MHz, $CDCl_3$, T = 60 °C): δ = 132.1 (q), 67.9 (CH), 67.1 (CH). ESI MS: *m*/*z* (%): 300 (M^+, 43), 277 (48), 262 (59). Elem anal. Calcd (%) for $C_{12}H_8FeN_2S_2$: C, 48.01; H, 2.69; N, 9.33. Found: C, 48.22; H, 2.51; N, 9.20.

General Procedure for the Preparation of 1,1′-Bis(thioureido)[11]ferrocenophanes, 3 and 4. To a solution of 1,1′-bis(isothiocyanato)ferrocene **2** (0.1 g, 0.33 mmol) in freshly distilled dry THF (80 mL) was added dropwise a solution of the appropriate amine (1.0 mmol), in the same solvent (80 mL), under nitrogen. The solution was stirred for 3 h at room temperature, and the resulting orange solid was filtered, washed with diethyl ether, and recrystallized from CH_2Cl_2/diethyl ether (1:1) to give the appropriate 1,1′-disubstituted ferrocene derivative.

3. 0.103 g, 60%; mp 221−224 °C (dec). IR (Nujol): ν = 3321, 3082, 3047, 1690, 1592, 1557, 1339, 1294, 1196, 1166, 1098, 1054, 1038, 1020, 976, 938, 874, 794 cm^{-1}. ^1H NMR (300 MHz, [D_6]DMSO, at T = 60 °C): δ = 1.23 (d, 12H, J = 6.3 Hz), 3.08 (m, 2H), 4.02 (bs, 4H), 4.73 (bs, 4H), 4.82 (bs, 4H), 6.99 (s, 1H), 7.14 (s, 1H), 7.71 (s, 2H), 8.95 (s, 2H). ^{13}C NMR (75.3 MHz, [D_6]DMSO, T = 60 °C): δ = 22.9 (CH_3), 27.4 (CH), 42.9 (CH_2), 63.1 (CH), 63.9 (CH), 97.9 (q), 120.4 (CH), 121.8 (CH), 132.6 (q), 142.3 (q), 180.7 (q). ESI MS: *m*/*z* (%): 519 (M^+ − 1, 100). Elem anal. Calcd (%) for $C_{26}H_{32}FeN_4S_2$: C, 59.99; H, 6.20; N, 10.76. Found: C, 60.23; H, 6.03; N, 10.51.

4. 0.096 g, 67%; mp 230−233 °C (dec). IR (Nujol): ν = 3332, 3236, 3196, 1688, 1591, 1537, 1333, 1291, 1195, 1105, 1023, 970, 935, 874, 802 cm^{-1}. ^1H NMR (400 MHz, [D_6]DMSO at T = 80 °C): δ = 4.04 (bs, 4H), 4.68 (bs, 4H), 4.82 (d, 4H, ^3J = 5.6 Hz), 7.06 (d, 2H, ^3J = 7.2 Hz), 7.23−7.25 (m, 2H), 7.79 (s, 2H), 8.88 (s, 2H). ^{13}C NMR (100.4 MHz, [D_6]DMSO at T = 80 °C): δ = 45.7 (CH_2), 63.0 (CH), 63.7 (CH), 97.9 (q), 122.0 (CH), 123.9 (CH), 127.2 (CH), 139.2 (q), 180.9 (q). ESI MS: *m*/*z* (%): 435 (M^+ − 1, 100). Elem anal. Calcd (%) for $C_{20}H_{20}FeN_4S_2$: C, 55.05; H, 4.62; N, 12.84. Found: C, 55.30; H, 4.89; N, 12.71.

5. 0.147 g, 91%; mp 193−196 °C. IR (Nujol): ν = 3394, 3153, 1595, 1529, 1315, 1298, 1252, 1186, 1100, 1068, 982, 911, 736 cm^{-1}. ^1H NMR (200 MHz, $CDCl_3$): δ = 1.16 (d, 12H, ^3J = 6.8 Hz), 3.05 (m, 2H), 4.83 (d, 4H, J = 5.0 Hz), 6.08 (t, 2H), 7.02 (s, 1H), 7.16−7.26 (m, 7H), 7.39 (d, 4H, ^3J = 7.8 Hz), 7.75 (bs, 2H). ^{13}C NMR (50 MHz, $CDCl_3$): δ = 23.8 (CH_3), 28.8 (CH), 47.2 (CH_2), 123.0 (CH), 125.6 (CH), 127.6 (CH), 128.9 (CH), 130.4 (CH), 131.0 (q), 135.7 (q), 147.1 (q), 180.4 (q). ESI MS: *m*/*z* (%): 489 (M^+ − 1, 100). Elem anal. Calcd (%) for $C_{28}H_{34}N_4S_2$: C, 68.53; H, 6.98; N, 11.42. Found: C, 68.71; H, 7.26; N, 11.64.

Scheme 1

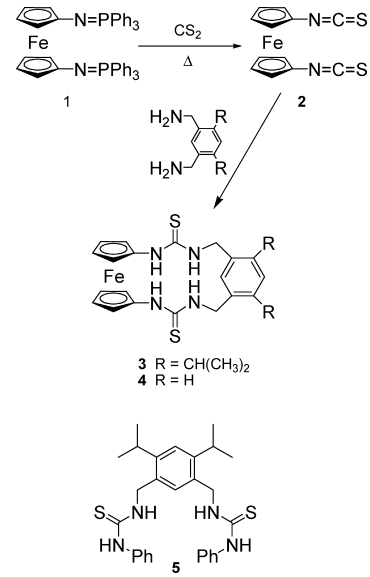

X-ray Data for Compound 3. $C_{26}H_{32}FeN_4S_2 \times 2$ DMF, M = 666.72, triclinic, space group $P\bar{1}$ (No. 2), a = 11.2153(3) Å, b = 12.7201(4) Å, c = 13.2468(4) Å, α = 109.900(2)°, β = 98.020(2)°, γ = 99.179(2)°, V = 1715.52(9) Å^3, T = 233(2) K, F(000) = 708, crystal size = 0.20 × 0.15 × 0.02 mm^3, Z = 2, Mo Kα (λ = 0.71073 Å), 9690 reflections collected, 5211 [R(int) = 0.0329] independent reflections, $wR2$ (all data) = 0.1299, goodness-of-fit is 1.056.

Crystallographic data for compound **3** reported in this paper have been deposited with the Cambridge Crystallographic Data Centre, CCDC 693271. Copies of this information may be obtained free of charge from The Director, CCDC, 12 Union Road, Cambridge CB2 1EZ, U.K. (Fax, +44-1223-336033; e-mail, deposit@ccdc.cam.ac.uk; or on-line, http://www.ccdc.cam.ac.uk).

Results and Discussion

Synthesis. The aza-Wittig reaction[18] of 1,1′-bis(*N*-triphenylphosphoranylidenamino)ferrocene **1**[3a] with CS_2 allowed the isolation of 1,1′-bis(isothiocyanato)ferrocene **2** in 25% yield after recrystallization (Scheme 1). The reaction of the bisheterocumulene **2** with 1,3-bis(aminomethyl)-4,6-diisopropylbenzene and *m*-xylylendiamine afforded the bis(thioureido)-[11]ferrocenophanes **3** and **4** in 60% and 67% yield, respectively. Likewise, and only for comparison purposes, the model compound **5** was prepared, in 91% yield, by reaction of 1,3-bis(aminomethyl)-4,6-diisopropylbenzene with phenylisothiocyanate. The ^1H and ^{13}C NMR spectra (which were recorded at 60 and 80 °C, respectively, because of the better resolution of peaks), elemental analyses, and mass spectra were consistent with the proposed structures (see the Experimental Section).

(15) Wiberg, K. *Tetrahedron* **1968**, *24*, 1083–1096.
(16) Bader, R. F. W. *Atoms in Molecules: A Quantum Theory*; Oxford University Press: Oxford, 1990.
(17) (a) AIM 2000 v. 2.0, designed by Biegler-König, F. W., and Schönbohm, J., 2002. Home page: http://www.aim2000.de/. Biegler-König, F.; Schönbohm, J.; Bayles, D. *J. Comput. Chem.* **2001**, *22*, 545–559. (b) Biegler-König, F.; Schönbohm, J. *J. Comput. Chem.* **2002**, *23*, 1489–1494.
(18) (a) Molina, P.; Alajarin, M.; Arques, A. *Synthesis* **1982**, 596–597. (b) Arques, A.; Molina, P. *Curr. Org. Chem.* **2004**, *8*, 827–843.

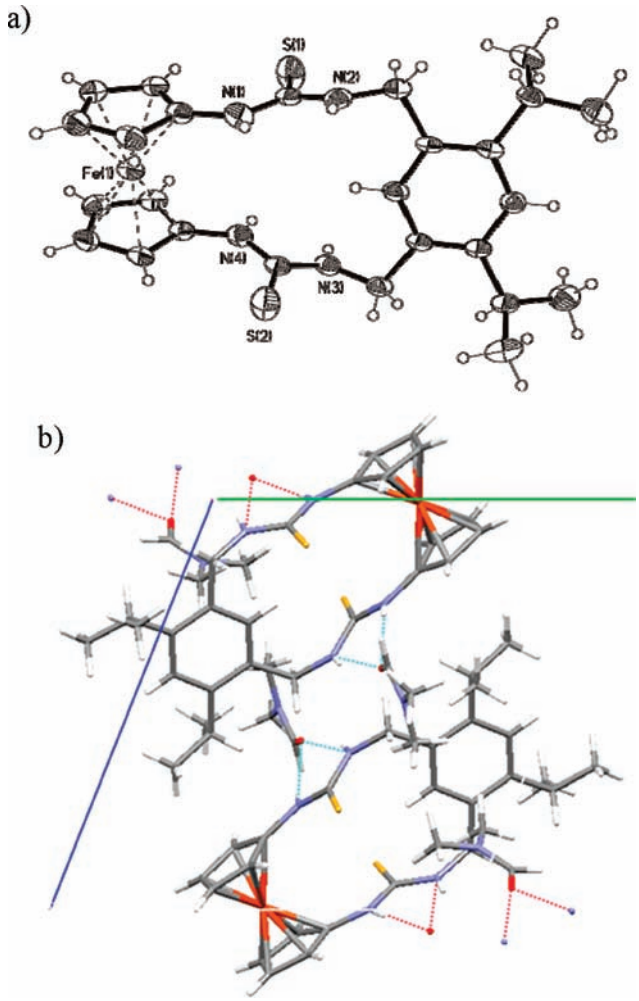

Figure 1. (a) Crystal structure of compound **3** (ORTEP molecular representation) and (b) crystal packing of compound **3** along the *a* axis, showing the intermolecular hydrogen bonds.

Additionally, single crystals of compound **3** were grown by slow evaporation of a dichloromethane solution containing 5% DMF for solubility, used for its X-ray crystal determination. An ORTEP view of compound **3** is shown in Figure 1. Compound **3** crystallizes in the triclinic space group $P\bar{1}$ with two molecules in the unit cell. The structure reveals almost eclipsed cyclopentadienyl rings with a dihedral angle of 7° between them because of the structure of the bis(thioureido) ring which shows a trans configuration of the two thiourea units. The 4,6-diisopropyl-*m*-xylylene unit is almost perpendicular to the cyclopentadienyl rings. The solid-state packing of compound **3** (Figure 1b) is best described as centrosymmetrically related pairs of molecules. Stacking of these related pairs occurs with a head-to-tail pairing. The relative arrangement and the large distances between neighboring molecules exclude the presence of hydrogen bonds among neighboring thiourea units, which instead form hydrogen bonds with the oxygen atom of the DMF solvent present in the crystal structure. Under these circumstances, the largest driving forces for such molecular packing are van der Waals and short $\pi\cdots$H−C and C−H$\cdots$N interactions, which lead to an efficient space filling.

We have also obtained the structure of the simplest ferrocenophane of this series, **4**, as well as the complex

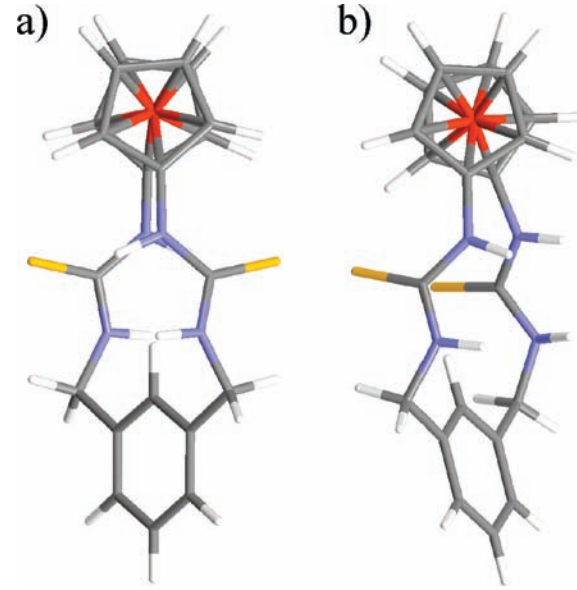

Figure 2. Calculated (mPW1B95/aug6-311G**) structures for (a) $\mathbf{4}^{C2}$ and (b) $\mathbf{4}^{qCs}$.

4·$(DMF)_2$ by means of quantum chemical calculations at the DFT level of theory, to check the performance of the selected computational level and its applicability in the study of its binding ability toward several anions and metal salts. The quality of several basis sets was checked by comparison of the calculated geometries of **4**·$(DMF)_2$ using two different functionals, with that determined by single-crystal X-ray diffraction for **3**·$(DMF)_2$ after replacing the iso-propyl groups by H atoms. Even with the standard B3LYP functional, the agreement with the experimental data (see the Computational Details) is remarkable[19] and systematically enhanced when using the hybrid meta functional mPW1B95.[10] Quantum chemical calculations performed on **4** also revealed the existence of a minimum energy conformation $\mathbf{4}^{qCs}$ (Figure 2a) with both thiourea groups pointing to the same side of the molecule (quasi-*Cs* symmetry). Either in solution or in the gas phase, this absolute minimum stationary point can be interconverted into a relative minimum structure with C_2-symmetry, $\mathbf{4}^{C2}$ (Figure 2b), by means of a transition state representing an energetic barrier of 12.70 kcal·mol^{-1}, low enough to allow moderately fast interconversion at room temperature, and featuring one of the thiourea groups almost parallel to the phane ring and with the NH groups pointing inward. The C_2-symmetric minimum is less stable by only 1.68 kcal·mol^{-1} but results in the preferred geometry in the crystalline state, probably because it enables a more compact packing.

Anion-Sensing Properties. At first, the electrochemical properties of receptors **3** and **4** on their own as well as in the presence of variable concentrations of F^-, Cl^-, Br^-, AcO^-, NO_3^-, HSO_4^-, $H_2PO_4^-$, and $HP_2O_7^{3-}$ as guest anionic

(19) Calculated RMSD in **4** 0.0844 Å at the B3LYP/aug6-311G** level of theory and 0.0793 and 0.0763 Å when using the mPW1B95 functional and aug6-31G* or aug6-311G** basis sets, respectively. These deviations reflect the fact that calculations do not take into account the crystal packing.

Table 1. Voltammetric Data of the Free Receptors **3** and **4** and Their Anionic Complexes Obtained in DMSO at 278 K

receptor[a]	$E_{1/2}$ (V)	$\Delta E_{1/2}$ (V)	E_a[b] (V)	K_{red}/K_{ox}[c]
3	−0.18			
3·AcO^-	−0.33	−0.15	0.09	343
3·$H_2PO_4^-$	−0.30	−0.12	0.09	107
3·$HP_2O_7^{3-}$	−0.33	−0.15	0.11	343
3·F^-	−0.27	−0.09	0.12	33
4	−0.22			
4·AcO^-	−0.39	−0.17	0.06	748
4·$H_2PO_4^-$	−0.37	−0.15	0.05	343
4·$HP_2O_7^{3-}$	−0.42	−0.20	0.04	2405
4·F^-	−0.34	−0.12	0.04	107

[a] Anions added as their tetrabutylammonium salts. [b] Anodic peak potential of the irreversible wave. [c] See refs 23 and 24.

species were investigated using CV and OSWV.[20] Each free receptor exhibited a reversible one-electron redox wave[21] typical of a ferrocene derivative, at the half-wave potential values shown in Table 1, calculated versus the ferrocenium/ferrocene (Fc^+/Fc) redox couple, which are identical to those obtained from the corresponding OSWV peaks (see the Supporting Information). The acyclic thiourea **5**, where the ferrocene moiety has been replaced by two phenyl groups, has been prepared and studied to determine the electrochemical behavior of the thiourea units present in this kind of receptors. However, the OSWV of the model compound **5** does not show any electrochemical process within the range in which all voltammetric experiments have been carried out ($E = -0.4$ to 0.4 V vs Fc^+/Fc).

Titration studies, with the addition of several anions as their tetrabutylammonium salts (TBA^+) to an electrochemical solution of receptors **3** and **4** ($c = 1 \times 10^{-3}$ M) in the appropriate solvent, containing 0.1 M [*n*-Bu_4N]PF_6 as supporting electrolyte, demonstrate that while addition of F^-, AcO^-, $H_2PO_4^-$, and $HP_2O_7^{3-}$ anions to these receptors promotes remarkable responses, indicating the interaction of thiourea binding sites with these anions (see below), addition of Cl^-, Br^-, HSO_4^-, and NO_3^- anionic species had no effect on their CV and OSWV, even when present in a large excess (up to 1/10, receptor/anion, ratio; see the Supporting Information). Nevertheless, the results obtained in OSWV on the stepwise addition of substoichiometric amounts of the appropriate guest anionic species revealed the appearance of a second wave that shifted cathodically from −0.20 V for **4**·$HP_2O_7^{3-}$ to −0.09 V for **3**·F^- (Table 1; Figure 3). Surprisingly, at the end of the titration, a new irreversible oxidation wave at more anodic potential ($E_a = 0.09-0.12$ V for receptor **3** and 0.04−0.06 V for receptor **4**) also appeared in the voltammogram.

Linear sweep voltammetry experiments carried out in the complexes, which display the presence of two waves

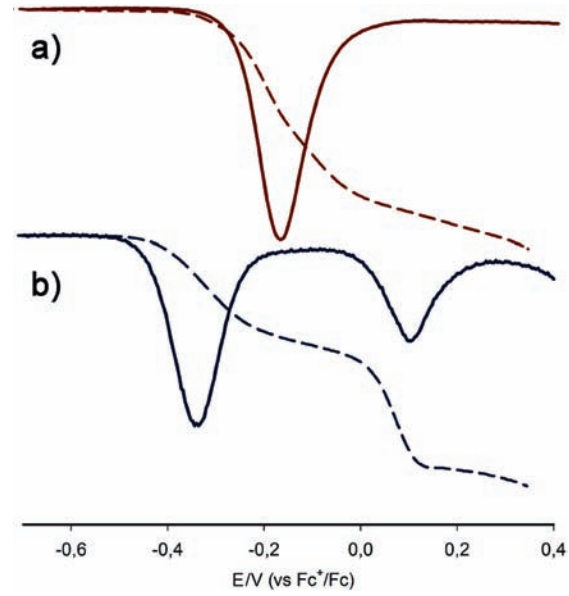

Figure 3. OSWV (solid lines) and linear sweep voltammetry (dashed lines) of (a) receptor **3** and (b) complex **3**·$HP_2O_7^{3-}$.

corresponding to anodic processes, have confirmed that the irreversible oxidation involves a one-electron process, as evaluated from the comparison of the heights of the Fe(II)/Fe(III) and irreversible oxidation waves (see the Supporting Information). Additionally, to elucidate the origin of the wave that appears at higher potential, studies of reversibility of the complexation process have been carried out. Addition of aqueous HBF_4 (5 or 6 equiv) recovered the original voltammogram, thus demonstrating the reversibility of the complexation.

In general, for receptor−anion systems exhibiting two-wave behavior, both half-wave potentials can be obtained from the voltammetric data as both redox couples are simultaneously detected, and then the binding enhancement factor (BEF)[22] could be calculated (Table 1). This factor, which defines the quantity K_{ox}/K_{red}, is deduced from the equation $\Delta E_{1/2} = (RT/nF)\ln(K_{red}/K_{ox})$.[23] Because K_{red} and K_{ox} correspond to the equilibrium constants for the complexation processes by the reduced and oxidized form of the ligands, this factor indicates the times that the complexation in the reduced form of the receptors is more difficult than that in the oxidized one.

On the other hand, the acyclic thiourea **5**, which, as it was mentioned before, did not show any electrochemical response upon addition of 5 equiv of the above-mentioned anions, gives rise to an oxidation process, with the appearance of a wave at $Ep = -0.23$ V. These results seem to confirm the fact that the waves exhibited by receptors **3** and **4** are related to the presence of the thiourea bridges in their structures (see the Supporting Information). We propose that this irreversible oxidation wave is due to the following: prior to the recognition process, the oxidation potential of the thiourea

(20) OSWV technique has been employed to obtain well-resolved potential information, while the individual redox processes are poorly resolved in the CV experiments in which individual $E_{1/2}$ potentials cannot be easily or accurately extracted from these data. (a) Serr, B. R.; Andersen, K. A.; Elliot, C. M.; Anderson, O. P. *Inorg. Chem.* **1988**, *27*, 4499–4504. (b) Richardson, D. E.; Taube, H. *Inorg. Chem.* **1981**, *20*, 1278–1285.

(21) The criteria applied for reversibility were a separation of 60 mV between cathodic and anodic peaks, a ratio for the intensities of the cathodic and anodic currents Ic/Ia of 1.0, and no shift of the half-wave potentials with varying scan rates.

(22) Beer, P. D.; Gale, P. A.; Chen, Z. *Adv. Phys. Org. Chem.* **1998**, *31*, 1–90.

(23) Richardson, D. E.; Taube, H. *Inorg. Chem.* **1981**, *20*, 1278–1285.

(24) Lo, K. K.-W.; Lau, J. S.-Y.; Fong, V. W.-Y. *Organometallics* **2004**, *23*, 1098–1106.

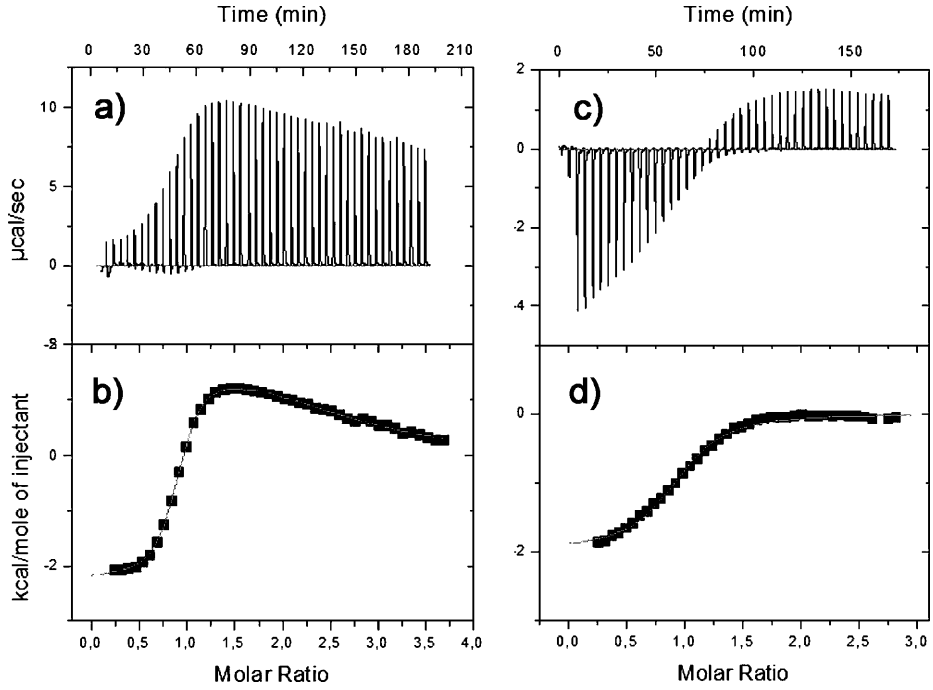

Figure 4. ITC titration plots of receptors **3** (left) and **4** (right) with $H_2PO_4^-$ (as TBA^+ salt). Top: raw data. Bottom: normalized integration data of the evolved heat per injection in terms of kcal mol^{-1} of injectant ($H_2PO_4^-$) plotted against the molar ratio ($H_2PO_4^-$/ligand).

fragment is higher than 1.3 V;[24] however, after the addition of the anion and the consequent formation of the anion−receptor hydrogen bonding complex, the oxidation potential of the thiourea group is reduced, making the oxidation more feasible.[25]

Isothermal titration calorimetry (ITC) provides useful insight into the nature of the binding interactions. It constitutes a method well suited for determining the affinity of a molecular guest toward an artificial host compound. Advantages of this method such as the capacity to elucidate the enthalpic and entropic components of the free energy for studying anion recognition properties have been recently reported.[26] ITC experiments were carried out by adding aliquots of the appropriate anion ($c = 1.4 \times 10^{-2}$ M) to a solution of the receptors **3** or **4** ($c = 1 \times 10^{-3}$ M) at 298 K in DMSO (see the Supporting Information). Typical ITC plots from the titration of **3** and **4** with the $H_2PO_4^-$ anion are depicted in Figure 4. The integration of the head pulses obtained in each titration step (Figure 4a,c) gives titration curves (Figure 4b,d) rendering the molar enthalpy $\Delta H°$ as the step height and the free energy $\Delta G°$ from the slope in the inflection point. The association constants, K_{as}, and the stoichiometry of complexation are derived as independent parameters from the fitting of curves, and finally, the molar $\Delta S°$ may be calculated from the Gibbs−Helmholtz equation. Considerably high affinities were found in the studied series of monocharged anions, and the resulting thermodynamic parameters and complexation data are collected in Table 2. Apart from F^- ion, which eludes the analysis as no significant heat effect was recorded in the titration, AcO^-, $H_2PO_4^-$, and $HP_2O_7^{3-}$ anions all showed well behaved responses.

Table 2. ITC Data[a] of Anionic Complexes Derived from Receptors **3** and **4**

receptor[a]	anion	K_{as}	L:A[b]	ΔH^c	$T\Delta S^c$	ΔG^c
3	AcO^-	6.4×10^3	1:1	−1.27	3.92	−5.19
3	$H_2PO_4^-$	4.19×10^5	1:1	−2.25	5.42	−7.67
		3.7×10^3	1:2	1.87	6.75	−4.88
3	$HP_2O_7^{3-}$	4.1×10^6	1:1	−4.34	4.69	−9.03
		9.3×10^4	1:2	−1.78	5.00	−6.78
4	AcO^-	2.4×10^3	1:1	−2.28	2.32	−4.60
4	$H_2PO_4^-$	2.1×10^4	1:1	−1.96	3.90	−5.86
4	$HP_2O_7^{3-}$	1.6×10^6	1:1	−4.85	3.64	−8.49
		1.0×10^5	1:2	−1.15	5.66	−6.81

[a] The solvent used was DMSO. [b] Ligand/anion stoichiometry. [c] kcal/mol^{-1}.

Large values for the complexation enthalpy and entropy were obtained from ITC measurements for AcO^-, $H_2PO_4^-$, and $HP_2O_7^{3-}$ anions, with both magnitudes being responsible for the exoergonic character of these complexations. The large positive values found for ΔS can be ascribed to the increase of disorder produced during the complexation by the replacement of the DMSO molecules in the solvation sphere of such anions. If one assumes that the solvation changes of anion complexation by **3** or **4** are similar because the core binding sites are identical, the much increased entropy contribution seen with receptor **3** would indicate a massive loosening of the host structure brought about by anion binding.

The experimental data points indicate the formation of a 1:1 complex for AcO^- anion and 1:2 for $HP_2O_7^{3-}$ anion. In the case of $H_2PO_4^-$ anion, a 1:1 binding model was found for receptor **4**, whereas in the titration with receptor **3** an exothermic primary 1:1 association step is followed by an

(25) Gunnlaugsson, T.; Fruger, P. E.; Lee, T. C.; Parkesh, R.; Pfeffer, F. M.; Hussey, G. M. *Tetrahedron Lett.* **2003**, *44*, 6575–6578.
(26) (a) Schmidtchen, F. P. *Org. Lett.* **2002**, *4*, 431–434. (b) Tobey, S. L.; Anslyn, E. V. *J. Am. Chem. Soc.* **2003**, *125*, 14807–14815. (c) Lee, C.-H.; Na, D.-D.; Yoon, D.-W.; Won, D.-H.; Cho, W. S. V.; Lynch, M.; Shevchuk, S. V.; Sessler, J. L. *J. Am. Chem. Soc.* **2003**, *125*, 7301–7306. (d) Sambrook, M. R.; Beer, P. D.; Wisner, R. L.; Paul, R. L.; Cowly, A. R.; Szemes, F.; Drew, M. G. B. *J. Am. Chem. Soc.* **2005**, *127*, 2292–2302. (e) Sessler, J. L.; An, D.; Cho, W.-S.; Lynch, V. M.; Marquez, M. *Chem. Eur. J.* **2005**, *11*, 2001–2011.

endothermic event of lower affinity (Figure 4b). This lower affinity binding step shows the ordinary pattern of ion-pairing in a polar solvent,[27] that is, a highly positive entropy in connection with a weak positive enthalpy (Table 2).

Free energy contributions in the anion complexation of hosts **3** and **4** must have two sources. One must come from the binding of the anions with the DMSO and another from the binding of the host with the anions. Insights about these two contributions can be obtained by inspecting the selectivity of the bisthiourea hosts **3** and **4** toward the anions. In view of the basicity of the anions, the selectivity should be in the order of AcO^- (pK_a AcOH = 4.74) > $H_2PO_4^-$ (pK_a H_3PO_4 = 2.12) > $HP_2O_7^{3-}$ (pK_a = 0.85 $H_4P_2O_7$). However, the ferrocenophane hosts bind $HP_2O_7^{3-}$ more strongly than $H_2PO_4^-$ and AcO^-. This tendency has also been observed for cyclic thioureas.[28] Accordingly, the observed selectivity $HP_2O_7^{3-}$ > $H_2PO_4^-$ > AcO^- must be due to the difference between the solvation of DMSO to the anions. It has been well documented that polar aprotic solvents such as DMSO are capable of electron-pair donation (Lewis basic) but are not very effective on the Lewis acidity scale. Thus for AcO^-, $H_2PO_4^-$, and $HP_2O_7^{3-}$ anions, the DMSO must stabilize the positively polarized atoms of the anions (i.e., carbon and phosphorus, respectively), rather than the negatively charged oxygen atoms. However, because the positively polarized phosphorus atoms of $H_2PO_4^-$ and $HP_2O_7^{3-}$ anions are surrounded by four oxygen atoms, they cannot be effectively solvated by DMSO. On the contrary, the corresponding carbon atom of the AcO^- anion must be more accessible to the solvation by DMSO, as revealed by previous thermodynamic data (ΔG_{solv} of AcO^- in DMSO = −62.7 kcal/mol).[29] Accordingly, the comparatively lower binding constant observed for AcO^- anion than those for $H_2PO_4^-$ and $HP_2O_7^{3-}$ anions can be attributed to the stronger interaction of the former with the solvent than that of the phosphorus-based anions.

^{1}H NMR titration experiments were also used to monitor the anion recognition process. Thus, thiourea receptors **3** and **4** were found to bind F^-, AcO^-, $H_2PO_4^-$, and $HP_2O_7^{3-}$ anions in DMSO solution ($c = 5 \times 10^{-3}$ M in DMSO-d_6) as evidenced by significant changes to the ^{1}H NMR spectrum of each receptor upon addition of such set of guest anions.

As expected, large downfield shifts in the resonance for the two N−H thiourea protons were observed upon the addition of aliquots of F^-, AcO^-, $H_2PO_4^-$, and $HP_2O_7^{3-}$ anions to the receptors **3** and **4** (see Table 2 and Figures 14−21 in the Supporting Information). This fact clearly demonstrates that the thiourea moiety is involved in the receptor−anion binding event (see Figure 5 and Supporting Information), suggesting the formation of complexes in which both thiourea arms are involved. As a consequence,

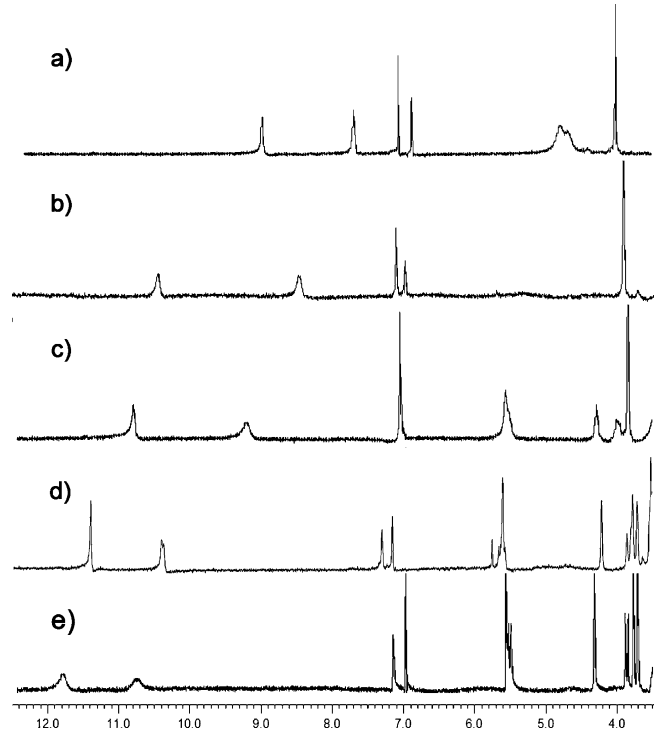

Figure 5. Partial ^{1}H NMR spectrum in DMSO-d_6 of (a) free receptor **3**, (b) **3** and 2 equiv of AcO^-, (c) **3** and 2 equiv of $H_2PO_4^-$, (d) **3** and 2 equiv of F^-, and (e) **3** and 2 equiv of $HP_2O_7^{3-}$.

the formation of such bonds rigidified the receptor, which is responsible for the shifts also observed in the methylene, ferrocene, and H-2 aromatic proton signals upon complexation. It should be highlighted that the presence of the thiourea peaks in the spectra of complexes is clear evidence that the ligands are not deprotonated by the anions and that the chemical and spectroscopical changes are caused by the coordination of the anions. All of these results confirm the formation of strong complexes between ligands **3** and **4** and the anions, showing also a good selectivity toward F^-, $HP_2O_7^{3-}$, $H_2PO_4^-$, and AcO^- anions.

To confirm the nature of these complexes, electrospray mass spectrometry experiments were registered on the complexes formed upon the addition of F^-, $HP_2O_7^{3-}$, $H_2PO_4^{2-}$, and AcO^-. The detection of the peak corresponding to the complex was possible only in the case of the complex with the largest association constant, $HP_2O_7^{3-}$. In all other cases, the free receptor peak was found. The mass spectrum of **3** with $HP_2O_7^{3-}$ exhibits a peak (m/z = 938, 100%) assigned to the complex $[\mathbf{3}\cdot H_2P_2O_7\cdot(C_4H_9)_4N]^-$, and the mass spectrum of **4** with $HP_2O_7^{3-}$ shows a peak (m/z = 854, 44%) assigned to the complex $[\mathbf{4}\cdot H_2P_2O_7\cdot(C_4H_9)_4N]^-$ accompanied with the peak of the free receptor (m/z = 436, 100%; see the Supporting Information). The observation of both complexes with the $HP_2O_7^{3-}$ anion is in accordance with the largest ΔG changes observed for such an anion from ITC measurements.

Binding of the aforementioned anions by the action of the simplest receptor **4** has also been modelized by means of DFT-based calculations. Under the working conditions, that is, using naked anions (no countercation was explicitly included) in the modelization, unless otherwise being stated,

(27) (a) Rekharsky, M.; Inoue, Y.; Tobey, S.; Metzger, A.; Anslyn, E. *J. Am. Chem. Soc.* **2002**, *124*, 14959–14967. (b) Jadhav, V. D.; Schmidtchen, F. P. *Org, Lett.* **2005**, *7*, 3311–3314. (c) Valik, M.; Kral, V.; Hertweck, E.; Schmidtchen, F. P. *New J. Chem.* **2007**, *31*, 703–710.

(28) (a) Bühlmann, P.; Nishizaya, S.; Xiao, K. P.; Umezawa, Y. *Tetrahedron* **1997**, *53*, 1647–1654. (b) Sasaki, S.; Mizuno, M.; Naemura, K.; Tobe, Y. *J. Org. Chem.* **2000**, *65*, 275–283.

(29) Pliego, J. R., Jr.; Rivero, J. M. *Chem. Phys. Lett.* **2002**, *355*, 543–546.

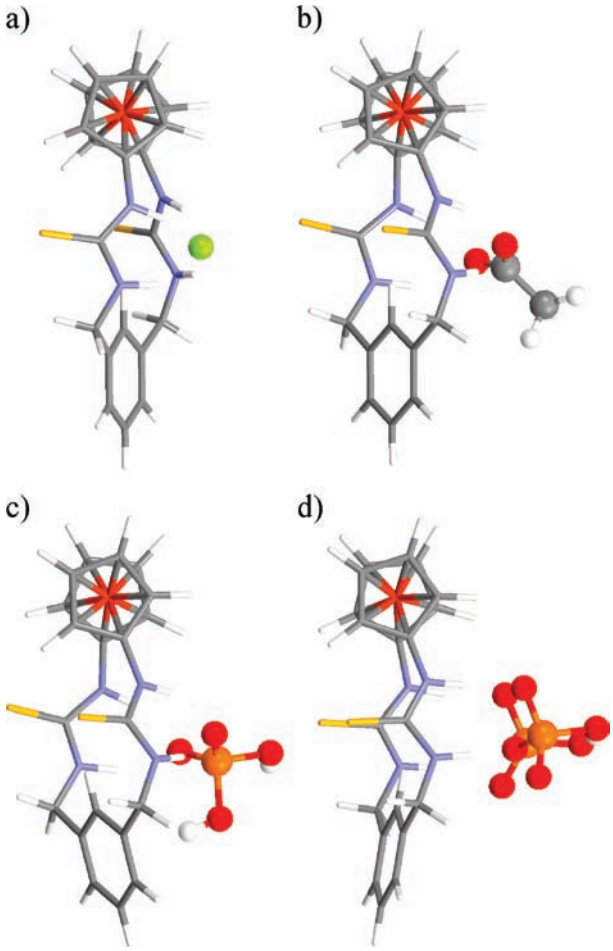

Figure 6. Calculated (mPW1B95/aug6-311G**) structures for (a) $[\mathbf{4}\cdot F]^-$, (b) $[\mathbf{4}\cdot OAc]^-$, (c) $[\mathbf{4}\cdot H_2PO_4]^-$, and (d) $[\mathbf{4}\cdot HP_2O_7.TMA_2]^-$ with TMA^+ cations omitted for clarity. The ligand is displayed in capped sticks while the guest is highlighted in a ball-and-stick representation.

optimizations were carried out in the gas phase, observing in all cases that 1:1 ligand/anion complexes derived from the most stable receptor $\mathbf{4}^{qCs}$ (Figure 6) resulted to be more favored than those derived from the other isomer $\mathbf{4}^{C2}$ (see the Supporting Information).

It is worth mentioning that in no case ligand deprotonation was observed in agreement with experimental (^{1}H NMR) evidence. Instead, the four thiourea NH groups of the ligand are oriented in a convergent fashion toward the hydrogen-acceptor atoms of the anionic guests that result partially wrapped. Strong interaction with the anionic guests is evidenced by the high value of the total WBI[15] extended over all ligand−anion contacts (Table 3), which favorably compares to those calculated as a reference for the dimers of hydrogen fluoride (0.024), water (0.025), or ammonia (0.017) at the same level. We have also used the Bader's AIM methodology[16] to perform a topological analysis of the electronic charge density, $\rho(r_c)$, to search for significant bond critical points (BCPs) around the spatial region where the noncovalent host−guest interactions are taking place. Indeed, the sets of four hydrogen bonds so far described for every ligand−anion complex can be appropriately characterized by their respective BCPs (Table 3) whose electron density, $\rho(r_c)$, agrees with the proposed relatively high bond strength, in comparison to hydrogen bonds in model small molecules.[30] Also, the relatively large positive $\nabla^2\rho(r_c)$ values found are usually a good diagnostic for the ionic character of the bonds.[31]

In all four receptor−anion complexes, we have also found three or four additional hydrogen bonds located within the receptor part that connect the thiocarbonyl groups with the H atoms belonging to either the Cp rings or the CH_2 groups adjacent to the *m*-phenylene moiety (Figure 6). As also outlined for the experimental X-ray structure of **3**, the calculated uncomplexed receptor $\mathbf{4}^{qCs}$ already shows these intramolecular hydrogen bonds,[32] thus explaining its high preorganization and therefore the low energetic cost to be paid for its adaptation upon complexation (ligand strain) with most of the anionic guests.

Cation-Sensing Properties. The presence of sulfur atoms in the molecule drove us also to study the cation-binding ability of these receptors. Therefore, the metal recognition properties toward Li^+, Na^+, K^+, Mg^{2+}, Ca^{2+}, Ni^{2+}, Cd^{2+}, Zn^{2+}, Pb^{2+}, and Hg^{2+} metal ions were evaluated by electrochemical analysis. In DMSO, no perturbation of the OSWV of **3** and **4** was observed upon addition of Li^+, Na^+, K^+, Mg^{2+}, Ca^{2+}, Ni^{2+}, Cd^{2+}, Zn^{2+}, and Pb^{2+} metal ions. However, on addition of Hg^{2+} ions to receptors **3** and **4**, the original wave decreases in intensity while a new wave appears at a more anodic potential. In the case of receptor **3**, the new wave appears at $E_{1/2} = 0.002$ V ($\Delta E_{1/2} = 184$ mV; BEF = 1290) with the addition of 1.5 equiv of Hg^{2+}, whereas for receptor **4**, it appears at $E_{1/2} = 0.038$ V ($\Delta E_{1/2} = 272$ mV; BEF = 39650) when 2 equiv of this cation were added (Figure 7).

The interference in the selective response of ligands **3** and **4** in the presence of Hg^{2+} metal ions from the other metal cations tested was also studied by using cross-selectivity experiments. Thus, addition of 1 equiv of Li^+, Na^+, K^+, Ca^{2+}, Mg^{2+}, Cd^{2+}, Ni^{2+}, Zn^{2+}, or Pb^{2+} cations in CH_3CN to 1 equiv of the receptors **3** or **4** in DMSO did not give any optical response. However, further addition of 1 equiv of Hg^{2+} to the above-mentioned solutions gave an identical optical response to that observed upon addition of 1 equiv of Hg^{2+} to a solution containing only 1 equiv of the appropriate ligand and which is free of the other metal cations (see the Supporting Information). These results clearly demonstrate

(30) Calculated hydrogen bonds X−H···X in dimers of model small molecules are as follows: for $\mathbf{(HF)_2}$, $d_{H\cdots F} = 1.850$ Å, WBI 0.024, $\rho(r_c) = 2.39 \times 10^{-2}$ e/a_0^3, and $\nabla^2\rho(r_c) = 9.98 \times 10^{-2}$ e/a_0^5; for $\mathbf{(H_2O)_2}$, $d_{H\cdots O} = 1.943$ Å, WBI 0.025, $\rho(r_c) = 2.48 \times 10^{-2}$ e/a_0^3, and $\nabla^2\rho(r_c) = 8.86 \times 10^{-2}$ e/a_0^5; for $\mathbf{(NH_3)_2}$, $d_{H\cdots N} = 2.252$ Å, WBI 0.017, $\rho(r_c) = 11.65 \times 10^{-2}$ e/a_0^3, and $\nabla^2\rho(r_c) = 14.92 \times 10^{-2}$ e/a_0^5. For comparison, the calculated covalent bonds X−H···X in dimers of the same model small molecules: for $\mathbf{(HF)_2}$, $d_{F-H} = 0.938$ Å, WBI 0.673, $\rho(r_c) = 0.350$ e/a_0^3, and $\nabla^2\rho(r_c) = -2.567$ e/a_0^5; for $\mathbf{(H_2O)_2}$, $d_{O-H} = 0.979$ Å, WBI 0.750, $\rho(r_c) = 0.347$ e/a_0^3, and $\nabla^2\rho(r_c) = -2.318$ e/a_0^5; for $\mathbf{(NH_3)_2}$, $d_{N-H} = 1.028$ Å, WBI 0.838, $\rho(r_c) = 0.323$ e/a_0^3, and $\nabla^2\rho(r_c) = -1.425$ e/a_0^5.

(31) Nakanishi, W.; Nakamoto, T.; Hayashi, S.; Sasamori, T.; Tokitoh, N. *Chem. Eur. J.* **2007**, *13*, 255–268, and references cited therein.

(32) For $\mathbf{4}^{qCs}$ $d_{CS\cdots HCp} = 2.909$ Å, WBI = 0.002, $\rho(r_c) = 0.55 \times 10^{-2}$ e/a_0^3, $\nabla^2\rho(r_c) = 1.61 \times 10^{-2}$ e/a_0^5; $d_{CS\cdots HCp} = 2.785$ Å, WBI = 0.003, $\rho(r_c) = 1.15 \times 10^{-2}$ e/a_0^3, $\nabla^2\rho(r_c) = 3.57 \times 10^{-2}$ e/a_0^5; $d_{CS\cdots HCAr} = 2.560$ Å, WBI = 0.019, $\rho(r_c) = 1.78 \times 10^{-2}$ e/a_0^3, $\nabla^2\rho(r_c) = 5.18 \times 10^{-2}$ e/a_0^5; and $d_{CS\cdots HCAr} = 2.530$ Å, WBI = 0.023, $\rho(r_c) = 1.85 \times 10^{-2}$ e/a_0^3, $\nabla^2\rho(r_c) = 5.30 \times 10^{-2}$ e/a_0^5.

Table 3. Relevant Calculated Parameters Related to the Complexing Behavior of **4** towards Anions (A) and Metal Salts (MA_n)

	$[\mathbf{4}^{qCs}\cdot F]^-$	$[\mathbf{4}^{qCs}\cdot OAc]^-$	$[\mathbf{4}^{qCs}\cdot H_2PO_4]^-$	$[\mathbf{4}^{qCs}\cdot HP_2O_7]^{3-}$ [a]	$[\mathbf{4}^{C2}\cdot(HP_2O_7)_2]^{6-}$ [a]	$\mathbf{4}^{qCs}\cdot Hg(OTf)_2$
$d_{NH\cdots A}$ [b]	1.604	1.770	1.840	1.801		1.860
	1.724	1.896	1.875	1.823	1.822[e]	1.897
	1.918	1.934	1.897	2.007	2.069	1.986
	2.057	2.015	1.945	2.151		2.005
$\sum WBI_{L\cdots A}$	0.311	0.213	0.188	0.216	0.266	0.170
$\rho(r_{c[NH\cdots A]})$ [c] $(\nabla^2\rho(r_{c[NH\cdots A]})$ [d]	5.43 (16.36)	4.14 (11.71)	3.36 (11.14)	3.64 (11.38)		3.16 (10.52)
	4.09 (13.29)	2.90 (9.88)	3.08 (10.58)	3.54 (10.84)		2.96 (10.02)
	2.65 (8.98)	2.61 (9.33)	2.94 (10.24)	2.39 (7.48)	4.04 (8.89)[e]	2.39 (8.26)
	2.03 (6.71)	2.21 (7.89)	2.54 (9.16)	1.81 (5.57)	2.05 (7.11)	2.24 (8.17)
$\sum \rho(r_{c[L\cdots A]})$ [c]	14.20	11.86	12.44	12.46	14.90	12.49
$\sum \rho^2\rho(r_{c[L\cdots A]})$ [d]	45.34	38.81	42.73	38.87	41.12	42.68
$d_{CS\cdots M}$ [b] $(WBI_{Cs\cdots M})$						2.470 (0.451)
						2.471 (0.448)
$\rho(r_{c[Cs\cdots M]})$ [c] $(\nabla^2\rho(r_{c[Cs\cdots M]}))$ [d]						7.44 (13.10)
						7.44 (13.20)

[a] Every $HP_2O_7^{3-}$ anion bears two TMA cations. [b] In Å. [c] In $e/a_0^3 \times 10^2$. [d] In $e/a_0^5 \times 10^2$. [e] Formal (covalent) N···H bond resulting from deprotonation by the pyrophosphate anion ($d_{O-H} = 1.012$ Å, WBI = 0.621, $\rho(r_c) = 0.3056$, e/a_0^3; $\nabla^2\rho(r_c) = -1.9136$ e/a_0^5).

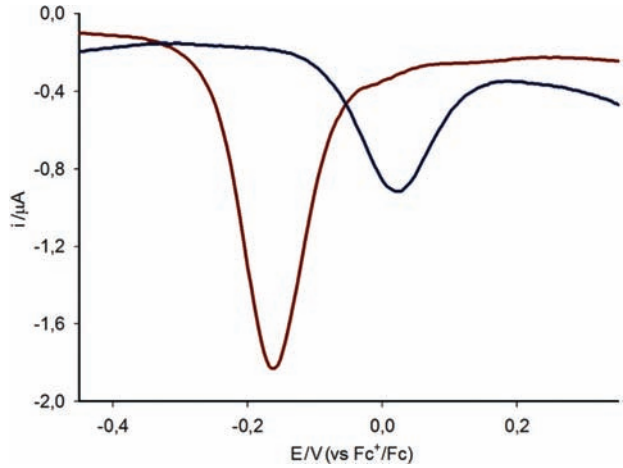

Figure 7. OSWV of **3** in DMSO/$[(n\text{-}Bu)_4N]PF_6$ (0.1 M) before (red) and after (blue) the addition of Hg^{2+} (as triflate salt).

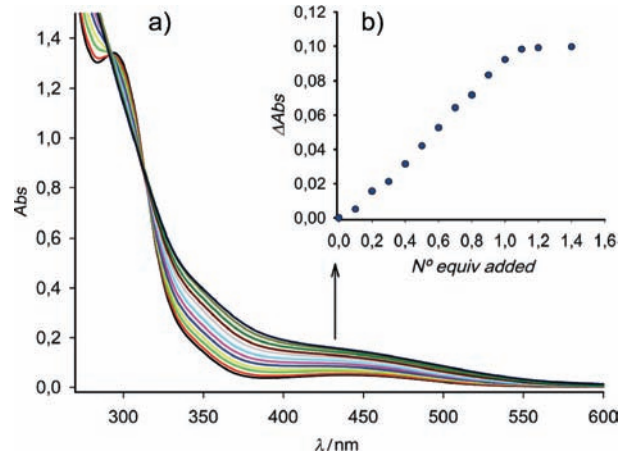

Figure 8. (a) Variation of the UV−vis spectrum of **3** ($c = 1 \times 10^{-4}$ M) in DMSO and (b) UV−vis titration curve, obtained upon addition of increasing amounts of Hg^{2+} (as triflate salt).

that these receptors have an excellent affinity for Hg^{2+} over those ions. The demand for sensing Hg^{2+} metal ions in competitive media such as DMSO is growing rapidly.[33]

Previous studies on ferrocene-based ligands have shown that bands ascribed to the lowest energy metal−ligand transitions (LE bands) in the absorption spectra are perturbed upon complexation.[34] Therefore, the metal recognition properties of the thiourea-metallocene dyads **3** and **4** were evaluated, additionally, by using UV−vis spectrophotometry with the set of cations previously mentioned. Titration experiments for DMSO solutions of these ligands ($c = 1 \times 10^{-4}$ M) and the corresponding ions were performed and analyzed quantitatively.[35] No changes were observed in the UV−vis spectra upon addition of Li^+, Na^+, K^+, Mg^{2+}, Ca^{2+}, Ni^{2+}, Cd^{2+}, Zn^{2+}, or Pb^{2+} even when they were added in a large excess to the DMSO solutions of any of these ligands. However, significant spectrophotometric changes in the metal−ligand absorption bands were observed on addition of increasing amounts of Hg^{2+} metal ions.

For both ligands **3** and **4**, the most prominent features observed during the complexation processes are the progressive increase of the corresponding metal−ligand transition band and the appearance of well-defined isosbestic points (Figure 8a), indicative of the presence, in the solution, of only two absorbing species in equilibrium: the free ligand (**L**) and the complex ($\mathbf{L}\cdot Hg^{2+}$). Thus, addition of increasing amounts of a solution of Hg^{2+} in CH_3CN ($c = 2.5 \times 10^{-2}$ M) to a solution of **3** in DMSO ($c = 1 \times 10^{-4}$ M) caused a progressive increase of the band located at $\lambda = 439$ nm ($\varepsilon = 490$ M^{-1} cm^{-1}) accompanied with a small bathochromic

(33) Among other things, see: (a) Shunmugan, R.; Gabriel, G. J.; Smith, C. E.; Aamer, K. A.; Tew, G. N. *Chem. Eur. J.* **2008**, *14*, 3904–3907. (b) Diez-Gil, C.; Caballero, A.; Ratera, I.; Tárraga, A.; Molina, P.; Veciana, J. *Sensors* **2007**, 3481–3488. (c) Diez-Gil, C.; Martinez, R.; Ratera, I.; Tárraga, A.; Molina, P.; Veciana, J. *J. Mater. Chem.* **2008**, *18*, 1997–2002.

(34) (a) Marder, S. R.; Perry, J. W.; Tiemann, B. G. *Organometallics* **1991**, *10*, 1896–1901. (b) Coe, B. J.; Jones, C. J.; McCleverty, J. A.; Bloor, D.; Cross, C. J. *J. Organomet. Chem.* **1994**, *464*, 225–232. (c) Müller, T. J.; Netz, A.; Ansorge, M. *Organometallics* **1999**, *18*, 5066–5074. (d) Carr, J. D.; Coles, S. J.; Hassan, M. B.; Hurthouse, M. B.; Malik, K. M. A.; Tucker, J. H. R. *J. Chem. Soc., Dalton Trans.* **1999**, 57.

(35) Specfit/32 Global Analysis System, 1999−2004 Spectrum Software Associates (SpecSoft@compuserve.com). The Specfit program was acquired from Bio-logic, SA (www.bio-logic.info) in January 2005. The equation to be adjusted by non-linear regression, using the above mentioned software, was $\Delta A/b = \{K_{11}\Delta\varepsilon_{HG}[H]_{tot}[G]\}/\{1 + K_{11}[G]\}$, where H = host, G = guest, HG = complex, ΔA = variation in the absorption, b = cell width, K_{11} = association constant for a 1:1 model, and $\Delta\varepsilon_{HG}$ = variation of molar absorptivity.

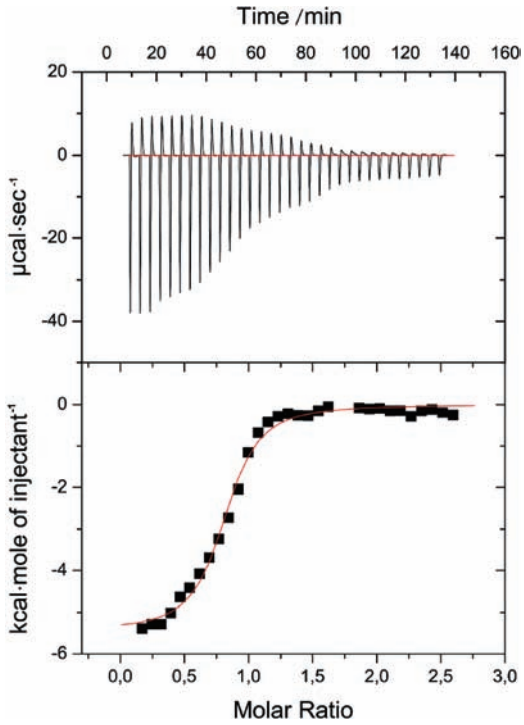

Figure 9. ITC titration plots of receptor **3** with Hg^{2+} (as triflate salt). Top: raw data. Bottom: normalized integration data of the evolved heat per injection in terms of kcal mol^{-1} of injectant (Hg^{2+}) plotted against the molar ratio (Hg^{2+}/ligand). To determine the values of the thermodynamic variables (ΔH, ΔG, and ΔS), the ITC data have been fitted to a 1:1 binding model.

shift ($\Delta\lambda = 6$ nm and $\Delta\varepsilon = 1010$ M^{-1} cm^{-1}). Two well-defined isosbestic points were found ($\lambda = 292$ and 313 nm), indicating that a neat interconversion between the uncomplexed and complexed species occurs. The resulting titration profile suggests a 1:1 ($\mathbf{L}\cdot Hg^{2+}$) binding model (Figure 8b). Similar results were obtained for ligand **4**, the detection limits being 2.3×10^{-5} M for both ligands.[36]

Furthermore, ITC studies have been carried out to calculate the association constants and the thermodynamic data related to the complexation process. The experiments were achieved by adding aliquots of the appropriate cation ($c = 7 \times 10^{-3}$ M) to a solution of the receptors **3** or **4** ($c = 1 \times 10^{-3}$ M) at 298 K in DMSO. The association constants (K_{as}) were calculated, as previously described, by nonlinear least-squares analysis of the data obtained from these ITC experiments, which also show that the recognition processes take place with a 1:1 stoichiometries ($\mathbf{L}\cdot Hg^{2+}$) and are also in agreement with the data previously obtained by the UV−vis titration experiments. The magnitudes of the corresponding association constants are 5.2×10^4 M^{-1} and 2.0×10^4 M^{-1} for ligands **3** and **4**, respectively. The thermodynamic data obtained show that for compound **3**, the complexation process is mainly enthalpy driven ($\Delta H = -5.45$ kcal/mol, $T\Delta S = 0.91$ kcal/mol, and $\Delta G = -6.36$ kcal/mol; Figure 9), while in the case of compound **4**, the driving forces are both enthalpy and entropy ($\Delta H = -1.96$ kcal/mol, $T\Delta S = 3.65$ kcal/mol, and $\Delta G = -5.61$ kcal/mol).

(36) Shortreed, M.; Kopelman, R.; Kuhn, M.; Hoyland, B. *Anal. Chem.* **1996**, *68*, 1414–1418.

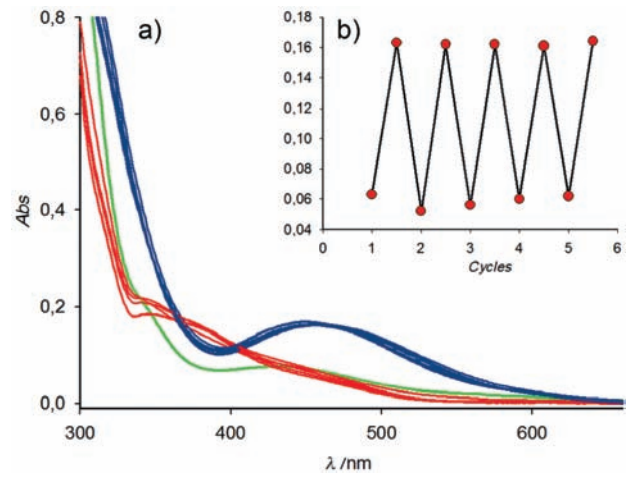

Figure 10. (a) UV−vis spectra recorded during the reversibility experiments carried out in CH_2Cl_2 for **3** with $Hg(CF_3SO_3)_2$ and (b) absorbance registered after each cycle.

The 1:1 stoichiometry of the complex formed between ligand **4** and Hg^{2+} cations was also confirmed by electrospray ionization mass spectrometry, in which three main peaks were observed: a strong peak because of the fragment $[(\mathbf{4}_2-2H)\cdot Hg]^+$ (44%) together with two peaks of higher intensity because of $[\mathbf{4}\cdot Hg]^+$ (100%) and $[(\mathbf{4}-1H)]^+$ (98%), respectively.

For the reported constants to be taken with confidence, we have proved the reversibility of the complexation process by performing the following experimental test: 1 equiv of $Hg(CF_3SO_3)_2$ was added to a solution of the ligand **3** in CH_2Cl_2 to obtain the complexed $\mathbf{3}\cdot Hg^{2+}$ species whose OSWV and UV−vis spectrum were recorded. The CH_2Cl_2 solutions of the complexes were washed several times with water until the color of the solution changed to that of the receptor. The organic layers were dried, the corresponding optical spectrum, OSWV, and ^1H NMR spectrum were recorded, and they were found to be the same as those of the corresponding free receptor **3**. Afterward, 1 equiv of $Hg(CF_3SO_3)_2$ was added to this solution, and the initial UV−vis spectrum and OSWV of the complex $\mathbf{3}\cdot Hg^{2+}$ were fully recovered. These experiments were carried out over several cycles, and the optical spectra were recorded after each step and found to be fully recovered on completion of the step, thus demonstrating the high degree of reversibility of the complexation/decomplexation processes (Figure 10). The lower solubility of **4** in CH_2Cl_2 prevented us from carrying out this experiment on this receptor.

The molecular structure of the complex which is formed upon addition of mercury(II) triflate to receptor **3** or **4** has been established with the aid of quantum chemical calculations. As described previously, we have used compound **4** as the only receptor model and assumed the 1:1 ligand/metal stoichiometry claimed as the most stable. The quasi-C_s stereoisomeric form of the receptor seems to be well suited for complexing oxoanionic salts of the soft highly thiophilic Hg^{2+} cation because of its two Janus-like faces. Thus the host simultaneously features an NH-rich surface for anion binding as previously described, furthermore contributing to increase the rigidity of the already preorganized ligand,

Figure 11. Calculated (mPW1B95/aug6-311G**/SDDecp) structure for complex $\mathbf{4}\cdot Hg^{2+}$. The ligand is represented in capped sticks while the guest is highlighted in a ball-and-stick representation. Counteranions are omitted for clarity.

whereas two thiocarbonyl groups on the other side lie almost parallel to each other and close enough ($d_{S\cdots S} = 4.559$ Å in the free receptor $\mathbf{4}^{qCs}$) to easily allow chelation of a Hg^{2+} cation. The calculated structure for [$\mathbf{4}\cdot Hg^{2+}$] (Figure 11) shows an almost planar-symmetric central receptor grabbing the Hg^{2+} ion with the tweezer-like thiocarbonyl groups. It is worth mentioning that the Hg^{2+} cation is essentially dicoordinated, as suggested by the almost linear S−Hg−S angle (155.3°), and does not promote oxidation of the ferrocene moiety as in related systems.[37] The interaction of the NH groups of the receptor with anions seems to increase the electron density at the central 1,3-phenylene C2 atom and consequently could enable it to behave as donor atom toward the Hg^{2+} cation.

The observed selectivity of receptor **4** toward Hg^{2+} in comparison to other metal cations has also been studied theoretically. With this aim, the structures of complexes [$\mathbf{4}^{qCs}\cdot M^{2+}$] for $M^{2+} = Cd^{2+}$ and Pb^{2+} were also obtained (see the Supporting Information), their formation being 8.6 and 21.7 kcal·mol^{-1} less stable, respectively, than that of Hg^{2+} at the working level of theory.

To study the mutual interference of anions and Hg^{2+} in the recognition ability of studied receptors, we also made competitive electrochemical experiments. Thus, the CV obtained upon addition of $HP_2O_7^{3-}$, $H_2PO_4^{2-}$, and AcO^- anions to an electrochemical solution of the $\mathbf{3}\cdot Hg^{2+}$ species showed that the first two molar equivalents of these anions have no affinity for the thiourea residues present in the complex $\mathbf{3}\cdot Hg^{2+}$. However, addition of three equivalents promotes the appearance of the redox wave ascribed to the free receptor **3**. Moreover, further additions of these anions (up to five equivalents) to such an electrochemical solution induced a cathodic shift of the redox wave, the magnitude of such a redox-potential being the same as that observed when those anions were added to the free receptor **3**. Thus, these results indicate that the added anions are apparently able to stoichiometrically bind the Hg^{2+} cation, avoiding their binding by the thiourea groups present in $\mathbf{3}\cdot Hg^{2+}$ host. It is also worth mentioning that a similar behavior was observed upon addition of the appropriate amounts of Hg^{2+} cation to the complexed species **3**·anion.

Conclusion

We have designed the first members of a potential class of easy-to-synthesize neutral ferrocenophane-based thiourea receptors and examined their binding properties toward various guest ions using electrochemical, spectral, and optical techniques, as well as by DFT-based quantum chemical calculations. Our synthetic methodology, which allows the preparation of ferrocenophane-based cyclic architectures, with the ferrocene unit directly linked to two thiourea groups, is based on the reaction of the 1,1′-bis(isothiocyanato)ferrocene **2** with diamino compounds. The rigidity of this new structural motif imposes two different binding sites (heteroionic-sensing Janus faces[38]): a sulfur-rich face as an ideal candidate to sense selectively the thiophilic Hg(II) metal cations and a face with four directional N−H bonds able to recognize anions. Selective binding to F^-, AcO^-, $H_2PO_4^-$, and $HP_2O_7^{3-}$ anions, in a polar solvent (DMSO) where hydrogen-bonding interaction between the thiourea functional groups and the anions is usually weakened by competing solvent molecules, was observed for these ferrocene-based thioureas. Remarkably, these receptors exhibit not only a high selectivity for Hg(II) cations over other cations with a strong anodic shift of the ferrocene oxidation wave ($\Delta E_{1/2} = 272$ mV) but also a significant change in the absorption spectrum. These new structural motifs pave the way to the design of a new generation of homoditopic receptors in which the ferrocene/ferrocenium redox couple and the ability of the thiourea moiety to act as binding site may operate cooperatively within the molecule. This synergistic relation may create a rare class of molecular systems which can behave as redox-switching homotopic receptors, with the dual capability of selectively sensing anions and cations.

Acknowledgment. We gratefully acknowledge the financial support from Fundación Séneca (Agencia de Ciencia y Tecnología de la Región de Murcia) Projects 02970/PI/05 and 04509/GERM/06 (Programa de Ayudas a Grupos de Excelencia de la Región de Murcia, Plan Regional de Ciencia y Tecnología 2007/2010), the DGI Spain Project CTQ2006-06333/BQU, and the Instituto Carlos III, MIyC, through "Acciones CIBER" Ciber BBN. This paper is dedicated to Prof. Josep Font Cierco, on the occasion of his retirement.

Supporting Information Available: Figures, tables of crystal data and structure refinement, and tables of the theoretical calculations. This material is available free of charge via the Internet at http://pubs.acs.org.

IC801879X

(37) Caballero, A.; Espinosa, A.; Tárraga, A.; Molina, P. *J. Org. Chem.* **2008**, *73*, 5489–5497.

(38) From the mythological roman god Janus, who is represented with a double-faced head, each looking in opposite directions.